



Published in final edited form as:

*Cancer Res.* 2017 July 01; 77(13): 3551–3563. doi:10.1158/0008-5472.CAN-17-0109.

## EGFR mediates responses to small molecule drugs targeting oncogenic fusion kinases

Aria Vaishnavi<sup>1,\*</sup>, Laura Schubert<sup>1</sup>, Uwe Rix<sup>2</sup>, Lindsay A. Marek<sup>3</sup>, Anh T. Le<sup>1</sup>, Stephen B. Keysar<sup>1</sup>, Magdalena J. Glogowska<sup>1</sup>, Matthew A. Smith<sup>4</sup>, Severine Kako<sup>1</sup>, Natalia J. Sumi<sup>2</sup>, Kurtis D. Davies<sup>5</sup>, Kathryn E. Ware<sup>3,+</sup>, Marileila Varella-Garcia<sup>1</sup>, Eric B. Haura<sup>4</sup>, Antonio Jimeno<sup>1</sup>, Lynn E. Heasley<sup>3</sup>, Dara L. Aisner<sup>5</sup>, and Robert C. Doebele<sup>1,\*</sup>

<sup>1</sup>Division of Medical Oncology, Department of Medicine, University of Colorado School of Medicine, Aurora, CO

<sup>2</sup>Department of Drug Discovery, H. Lee Moffitt Cancer Center and Research Institute, Tampa, FL

<sup>3</sup>Department of Craniofacial Biology, University of Colorado School of Dental Medicine, Aurora, CO

<sup>4</sup>Department of Thoracic Oncology, H. Lee Moffitt Cancer Center and Research Institute, Tampa, FL

<sup>5</sup>Department of Pathology, University of Colorado School of Medicine, Aurora, CO

### Abstract

Oncogenic kinase fusions of ALK, ROS1, RET and NTRK1 act as drivers in human lung and other cancers. Residual tumor burden following treatment of ALK or ROS1+ lung cancer patients with oncogene-targeted therapy ultimately enables the emergence of drug-resistant clones, limiting the long-term effectiveness of these therapies. To determine the signaling mechanisms underlying incomplete tumor cell killing in oncogene-addicted cancer cells, we investigated the role of EGFR signaling in drug-naïve cancer cells harboring these oncogene fusions. We defined three distinct roles for EGFR in the response to oncogene-specific therapies. First, EGF-mediated activation of EGFR blunted fusion kinase inhibitor binding and restored fusion kinase signaling complexes. Second, fusion kinase inhibition shifted adaptor protein binding from the fusion oncoprotein to EGFR. Third, EGFR enabled bypass signaling to critical downstream pathways such as MAPK. While evidence of EGFR-mediated bypass signaling has been reported after ALK and ROS1 blockade, our results extended this effect to RET and NTRK1 blockade and uncovered the other additional mechanisms in gene fusion-positive lung cancer cells, mouse models and human clinical specimens before onset of acquired drug resistance. Collectively, our findings show how

\* Correspondence to: Robert C. Doebele, 12801 E. 17<sup>th</sup> Ave, Aurora, CO 80045, Phone: 303.724.2980, Fax: 303.724.3889, robert.doebele@ucdenver.edu.

\* Present address: Huntsman Cancer Institute, University of Utah, Salt Lake City, UT.

+ Present address: Department of Molecular Genetics and Microbiology, Duke University Medical Center, Durham, NC.

### Conflicts of interest

Sponsored research agreements from Loxo Oncology, Igynta, Threshold Pharmaceuticals and Strategia to the University of Colorado (RCD). Consulting and/or honoraria from Ariad Pharmaceuticals, AstraZeneca, Pfizer, Guardant Health and Trovogene to RCD. PCT/US2013/057495 licensed by Abbott Molecular to RCD, MVG, and ATL. LEH has research grants from AstraZeneca, Ariad Pharmaceuticals and Servier and ad hoc consults for Merrimack Pharmaceuticals.

EGFR signaling can provide a critical adaptive survival mechanism that allows cancer cells to evade oncogene-specific inhibitors, providing a rationale to co-target EGFR to reduce risks of developing drug resistance.

## Keywords

gene fusion; kinase oncogenes; targeted therapies; lung cancer; combination therapy

---

## Introduction

Inhibition of oncogene fusions such as *ALK*, *ROS1*, *RET*, or *NTRK1* blocks cancer cell proliferation and survival, consistent with the model of oncogene addiction (1–3). *ALK*+ and *ROS1*+ patients treated with the inhibitor crizotinib demonstrate remarkable objective response rates and progression free survival times (4,5). Early evidence also supports the efficacy of targeting *TRK* and *RET* in lung cancer patients bearing oncogenic forms of these RTKs (6–8). These oncogenes result from genomic rearrangements, which generate expression of a chimeric protein with a constitutively activated kinase domain (9,10), herein referred to as a fusion kinase.

Complete tumor responses are rare following oncogene inhibition with tyrosine kinase inhibitors, suggesting that a large population of tumor cells survive inhibition of the dominant oncogene (11,12). Ultimately all patients will experience disease progression, most often from cellular resistance to the targeted therapies (13–15). The primary approach of most drug resistance studies has been to study tumor samples from progressing tumor lesions or by use of established cancer cell lines that have undergone long-term selective pressure under targeted therapy (13,14). These strategies have been valuable in determining acquired resistance mechanisms that arise from the outgrowth of drug resistant cancer cell clones. It has led to the development of next generation tyrosine kinase inhibitors (TKIs) that can overcome some mechanisms of acquired drug resistance such as kinase domain mutations, but do not yield insight into how to improve initial treatment with up-front combination therapy, an alternate approach to combat the development of drug resistance (16).

Analysis of depth of response using RECIST criteria from a combined cohort of *ALK*+ patients treated with an *ALK* inhibitor showed an association between greater individual patient tumor response and longer survival (17). Thus, an alternate approach to drug resistance would be to investigate the mechanisms that underlie the incomplete tumor response observed in the majority of patients who respond to oncogene-targeted therapy. Indeed, early adaptive signaling mechanisms could permit survival of a substantial number of cancer cells following the initial insult of a kinase inhibitor, resulting in the residual tumor burden observed in the majority of patients treated with oncogene-targeted therapy, and ultimately allowing the outgrowth of drug-resistant cancer cell clones (18,19). This particular study is focused on understanding signaling mechanisms used by cancer cells harboring oncogenic fusions that allow survival despite targeted inhibition.

EGFR is one of the most studied receptor tyrosine kinases (RTKs) because it plays an essential role during embryonic development and adult homeostasis and is often aberrantly activated in cancer (20). EGFR is expressed at high levels or mutated in many epithelial malignancies including lung, glioma, HCC, breast, colorectal, HNSCC, and ovarian cancers (20). Wild-type EGFR is an established therapeutic target in HNSCC, colorectal cancer, and squamous cell lung cancer and thus plays an important role in cancer cell signaling in these tumors (21–23). EGFR is overexpressed in ~80% of NSCLC and is associated with a poor prognosis, but most current clinical trials in this disease focus on targeting only those tumors that harbor drug-sensitizing EGFR mutations, not the majority of patient tumors that express high levels of the wild-type receptor (24).

The studies presented here investigated the role of wild-type EGFR signaling in cancer cells that harbor oncogenic fusion kinases prior to the onset of acquired drug resistance in an effort to improve our understanding of early adaptive cancer cell signaling that mediates survival in the face of oncogene inhibition. We evaluated potential roles for EGFR signaling following treatment with a fusion kinase inhibitor (FKI), but also in the absence of any therapeutic stress in fusion oncogene positive human-derived cancer cell lines, murine cancer models, and patient tumor samples. In this report, we describe multiple and distinct roles for EGFR signaling in drug naïve fusion kinase positive cancer cells, which indicate a novel role for EGFR as a cooperative signaling partner in these molecular subtypes.

## Materials and Methods

### Patients

Written informed consent was obtained from the patient prior to use of the patient's tumor sample. The consent form and protocol was reviewed and approved by the Colorado Multiple Institutional Review Board. Excess tumor tissue from patients was collected for derivation of tumor xenografts (COMIRB #10-1386) or for additional research studies (COMIRB #11-1621). Patient studies were conducted according to the Declaration of Helsinki, the Belmont Report, and the U.S. Common Rule.

### Cell lines and reagents

H3122, H2228, HCC78, H1650, H520, and H1993 (all obtained in 2008–2010 from Dr. Paul A. Bunn, University of Colorado), CUTO-3 (derived in 2013 by our laboratory), CUTO-2 (derived in 2012 by our laboratory), DFCI-032 (obtained in 2014 from Dr. Pasi A. Jänne, Dana Farber Cancer Institute), STE-1 (obtained in 2013 from Christine M. Lovly, Vanderbilt University) and KM12 (obtained in 2013 from Dr. Gail Eckhardt, University of Colorado) cell lines were previously described (1,13,15,25–27). LC-2/ad cells were purchased from Sigma-Aldrich in 2013 and 293T purchased from ATCC in 2009. All cancer cell lines were authenticated using DNA fingerprinting analysis by short tandem repeat profiling, subjected to routine mycoplasma testing and cultured in RPMI1640 supplemented with 1–10% FBS. 293-T cells were maintained in DMEM supplemented with 5% FBS. Gefitinib, crizotinib, and TAE-684 were purchased from Selleck chemicals. ARRY-470 was kindly provided by Array Biopharma, and foretinib (XL880) was kindly provided by GlaxoSmithKline. All EGF was purchased from R&D Systems. The following plasmids were previously described:

pCDH-EML4-ALK, pCDH-SDC4-ROS1, pCDH-MPRIP-NTRK1, pCDH-MPRIP-NTRK1-KN (1,13,15,28). The FGFR1 cDNA was obtained from Origene, and EGFR was cloned from the EGFR-EGFP expression plasmid from the Sorkin Lab (Addgene, plasmid #32751) and both were cloned into the PLVX plasmid.

### **Lentivirus shRNA production and cell transduction, and plasmid transfection**

293-T cell transient transfections were performed using Mirus TransIT LT1® or TransIT-X2® reagents according to the manufacturer's protocol. Mission Non-Target shRNA Control #SHC002 and 2 EGFR shRNAs were ordered from the Functional Genomics Facility at the University of Colorado (Boulder, CO) TRCN0000010329 (sh#1) and TRCN0000039634 (sh#2). EGFR shRNAs were transfected into 293T cells and stably transduced into CUTO-3 and LC-2/ad cells as previously described (1).

### **Co-Immunoprecipitations**

Cell lysates were obtained using a modified RIPA lysis buffer and incubated rotating overnight at 4°C with each designated antibody or antibody-bead conjugate (mouse EGFR sepharose beads, Cell Signaling, #8083). Lysate-antibody complexes were then incubated for 2 hours with PBS washed protein-G conjugated agarose beads at 4°C (Merck Millipore, catalog #539207.) Beads were washed through inversions and spun at 13k rpm for 30 seconds at 4°C 3× with ice cold PBS. Beads were re-suspended in sample loading buffer, boiled, and stored at –80°C prior to immunoblot analysis. Antibodies were used for immunoblot analysis as described below.

### **Biotin conjugated crizotinib pull-downs**

HCC78 or H3122 cells were incubated with PureProteome™ streptavidin conjugated magnetic beads (Millipore), following the specified drug or growth factor treatments, according to the manufacturer's protocol. Beads were washed 3× using a magnet, and re-suspended in sample loading buffer, boiled, and stored at –80°C prior to immunoblot analysis.

### **Immunoblotting**

Immunoblot analysis was performed as previously described (1). Precast 4–20% gradient gels (Bio-Rad) were used for EGFR and GRB2 immunoprecipitations. The following antibodies were used from Cell Signaling Technology: pTRK Y490 (9141 or 4619) and Y464/65 (C50F3), pEGFR Y1068 (D7A5) and Y1173 (53A5), total EGFR (2232L or XP D38B1), HA (C29F4 or 6E2), pALK Y1278/1282/1283 (3983), total ALK (D5F3, 3333, or 31F12), total ROS1 (D4D6), pRET Y905 (3221), total RET (C31B4), pERK1/2 XP T202/Y204, total ERK1/2 (3A7), pAKT S473 XP (D9E 4060 or 193H12), GRB2 (3972), and pan-keratin (C11). Total RET was also purchased from Abcam (ab134100), GAPDH (MAB374) and pTYR (4G10) from Millipore, total EGFR (610017) from BD Biosciences, total TRK (C-14) and Tubulin antibodies from Santa Cruz Biotechnology and FGFR1 antibody (#TA301021) was purchased from Origene.

## Proliferation assays

All proliferation assays were performed in media supplemented with 5% FBS as previously described using Cell Titer 96 MTS (Promega) (1). Cells were seeded at 750, 1000, or 2000 cells/well and treated for 72 hours at the drug concentrations indicated. Each assay was performed in triplicate and using at least 3 independent biological replicates. Data were graphed and analyzed using GraphPad Prism software, with 50% inhibitory concentrations (IC<sub>50</sub>) values calculated as half maximal response. The 9 cell lines assayed by MTS were additionally pooled together for statistical analysis. All statistical analysis was performed using a paired student's t test.

## Proximity Ligation Assays (PLAs)

Cells were seeded onto chamber slides at 25–50k cells/well. Cells were treated with the indicated doses and times then fixed for 15 minutes by shaking at room temperature in 4% paraformaldehyde. Cells were rinsed twice in PBS, and then the Duolink® In situ PLA ® kit (SigmaAldrich) in mouse/rabbit (with red detection) was used according to the manufacturer's protocol (catalog # DUO92002, 92004, 92008). Antibody concentrations were optimized prior to PLA experiments. FFPE tissue PLAs from murine cell line xenografts of patient-derived xenografts or patient tumor samples were prepared as described in histology. Additionally, FFPE samples were treated with 300mM glycine for 30 minutes prior to the blocking step, then the assay was performed according to the manufacturer's protocol. Cells were mounted using Duolink® In Situ Mounting Medium (with DAPI) and cured, and sealed with clear nail polish prior to imaging. Images were taken on a Nikon standard inverted fluorescent microscope at 40×. The following antibodies were used in the PLA: ALK (D5F3), RET (C31B4), ROS1 (D4D6), EGFR (D38B1), and Trk (C17F1) from Cell Signaling Technology or (C-14, SC-11) from Santa Cruz; SHC1 (3F4, H00006464) from Novus; Grb2 (26B04) from Invitrogen; Grb2 (610111) from BD Biosciences; EGFR (29.1, E2760) from Sigma-Aldrich; and EGFR (SC-120) and Grb7 (A-12) from Santa Cruz Biotechnology. The antibodies used in PLAs were tested for specificity using various control cell lines. A stage micrometer (reticles.com, KR-85-11) was imaged and the scale bar inserted into the images. Each scale bar shown represents 50 microns, unless stated otherwise.

## CellProfiler quantification of PLAs

At least 3 independent experiments and at least 300 nuclei were assayed in every quantification analysis. Cellprofiler software was used to quantify these assays (29). The pipeline used in these studies to analyze images was: ColorToGray (to split fluorescent channels), EnhanceorSuppressFeatures (to enhance the red speckles), IdentifyPrimaryObjects (to specify the number of nuclei in the blue channel), and MeasureImageIntensity (of speckles in the red channel) for each image. Red fluorescence intensity was normalized to the number of nuclei in each image field. Each quantification graph is expressed as the mean ± the SEM. All statistical analysis was performed using a paired student's t test.

## Fluorescence In-Situ Hybridization

*NTRK1* FISH assays were performed as previously described (1).

## Histology/Immunohistochemistry

Tumor specimens were fixed in 10% neutral buffered formalin, processed, paraffin-embedded and cut at 4 microns. Slides were stained with hematoxylin-eosin and examined microscopically. For IHC staining, the slides were de-paraffinized in xylene and rehydrated in graded concentrations of ethanol before antigen retrieval in EDTA pH 9 solution (Dako) in a pressure cooker at 121°F for 10 minutes. Next, the slides were cooled for 20 minutes before washing in 1× Wash Buffer (Dako). They were then treated with Dual Endogenous Enzyme Block (Dako) for 10 minutes, followed by Serum-Free Block (Dako) for 20 minutes. The samples were incubated with antibody for 60 minutes at room temperature (RT) followed by HRP-conjugated EnVision + Dual Link System (Dako). Staining was developed using DAB+ chromogen solution (Dako). Slides were counterstained with automatic hematoxylin (Dako), washed with wash buffer and distilled water, alcohol dehydrated and mounted with resinous media. EGFR D38B1 and pEGFR D7A5 from Cell Signaling were used. H-score analysis of EGFR IHC in patient samples was performed as previously described (30).

## Animals

Animal care and procedures were approved by the Institutional Animal Care and Use Committee Office of the University of Colorado Anschutz Medical Campus. Forty nu:nu male mice were injected with  $10^6$  H3122 cells in each flank subcutaneously. Mice were kindly provided a breeder colony run by Lynn Heasley and James DeGregori. Once tumors reached 250 mm<sup>3</sup>, mice were randomly distributed into 4 groups ( $n = \sim 20$  tumors/group) and treated daily by oral gavage with the following: diluent, crizotinib 50 mg/kg, gefitinib 25 mg/kg, or both for 17 days. Tumor size was measured twice weekly using calipers and tumor volume was calculated using the formula: volume = (length × width<sup>2</sup>)/2. Gefitinib was purchased from Selleck, and crizotinib was kindly gifted back to the Doebele lab from patients. Drugs were reconstituted in “diluent”, which was 1% polysorbate 80. Mice were sacrificed when tumor volume or appearance exceeded regulations, and tumor specimens were excised, fixed in neutral buffered formalin, paraffin-embedded, and slides cut at 4 microns. Each tumor was analyzed by the indicated PLA as pharmacodynamic markers. Final statistical comparisons of tumor volume change were calculated using ANOVA with Graphpad Prism software.

## Patient derived xenograft maintenance

Animal care and procedures were approved by the Institutional Animal Care and Use Committee Office of the University of Colorado Anschutz Medical Campus. Propagation and maintenance of CULC001 and CULC002 xenografts was previously described (6,31).

## Results

### EGFR augments downstream signaling and proliferation in fusion kinase+ cancer cells by amplifying fusion kinase activity

Previous studies from our lab have shown that EGFR mediated partial intrinsic resistance to targeted inhibition of ROS1 in a ROS1+ cell line, and EGFR mediated the acquired resistance in that cell line when treated chronically with a ROS1 FKI (13,28). Here, we observed incomplete inhibition of critical downstream signaling pathways in drug naïve gene fusion positive cell lines where the fusion kinase was inhibited pharmacologically (Fig. 1A, Supplementary Fig. S1). We hypothesized that EGFR could account for the incomplete inhibition in these cell lines. In support of this hypothesis, the addition of the EGFR-specific tyrosine kinase inhibitor (TKI), gefitinib, increased inhibition of downstream signaling pathways (Fig. 1A) while EGF stimulation had the opposite effect by rescuing phosphorylation of important downstream signaling pathways such as ERK1/2 and AKT in lung cancer cell lines bearing TRKA, RET, ROS1 and ALK fusions (Supplementary Fig. S1).

We also asked whether EGFR activation could influence constitutive fusion kinase signaling in the absence of inhibition by an FKI. We measured the kinetics of EGFR, fusion kinase, and ERK1/2 phosphorylation following EGF stimulation. We observed rapid, maximal activation of EGFR at 5 minutes and increased phosphorylation of the fusion kinases above levels that occur from its constitutive activation, which also resulted in further amplification of downstream signaling (Fig. 1B, Supplementary Fig. S1). These data provide evidence that the activity and signaling of oncogenic fusion kinases can be modified by non-oncogenic RTK signaling, such as EGFR, under normal constitutive signaling or FKI-treated conditions.

The ability of EGFR to regulate both fusion kinase phosphorylation and downstream signaling suggests an important role for this RTK in tumor cells. We therefore asked whether EGFR and its signaling regulated tumorigenic properties, such as cell proliferation in cancer cells harboring oncogenic fusions. We expanded upon our initial studies to include 9 different fusion kinase positive cell lines (Supplementary Table 1) to determine the influence of EGFR inhibition or activation on cellular proliferation in the presence of a cognate FKI (Fig. 1C). Inhibition of EGFR with gefitinib significantly increased the sensitivity of the cell lines to their respective FKIs by an average of 12.7-fold ( $P=0.01$ ), whereas stimulation of EGFR with EGF significantly decreased the sensitivity of the cells by 5.9-fold ( $P=0.004$ ), demonstrating an important role for EGFR signaling in cancer cells that express fusion oncogenes (Fig. 1C, Supplementary Table S1). It is notable that EGFR inhibitors had an effect on proliferation even in the absence of exogenous EGF, consistent with the downstream signaling results in Fig. 1A. Additionally, depletion of EGFR by RNAi enhanced FKI inhibition in TRK and RET models, further supporting the role of EGFR in proliferation of these cells (Supplementary Fig. S2).

## EGFR transactivates fusion kinases in lung cancer cells

After observing the effect of EGF stimulation on constitutive fusion kinase signaling, we tested whether EGFR activation could induce phosphorylation of the fusion kinase in the presence of an FKI. Although EGF-induced bypass signaling was anticipated, re-phosphorylation of the drug-inhibited fusion kinase was not expected (Fig. 2A, Supplementary Fig. S1). This result suggested an additional, unexplored role for EGFR signaling in cancer cells. Because EGFR signaling can transactivate a fusion kinase in an inactive state (FKI-bound), we asked whether EGFR could also transactivate a different type of inactive state of the fusion kinase: a catalytically inactive version of the fusion kinase. To address this, we co-expressed *EGFR* and kinase-dead, HA-tagged myosin phosphatase Rho-interacting protein (*MPRIP*)-*NTRK1* K544N fusion genes in 293T cells (1). EGF stimulation resulted in phosphorylation of the catalytically inactive RIP-TRKA protein, and this effect was abrogated with EGFR kinase inhibition (Fig. 2B). Similarly, EGFR-mediated transactivation was observed for the catalytically inactive mutant of *CD74-NTRK1* (Supplementary Fig. S1E).

To further understand the mechanism of fusion kinase re-phosphorylation, we tested whether EGF-induced activation of EGFR resulted in the dissociation of the FKI. To address this, we used a biotin-linked crizotinib or biotin-linked cabozantinib as a bait to pull down the drug and its target kinase, ROS1 or ALK, respectively, using streptavidin-conjugated beads (32). Biotin-labeled cabozantinib pulled down ROS1, and biotin-labeled crizotinib pulled down ALK, and the biotinylated drug-fusion kinase complex was lost upon competition with the addition of excess, unlabeled drug (Fig. 2C). Importantly, stimulation of cells with EGF also disrupted the biotin-cabozantinib pull down of ROS1 or biotin-crizotinib pull down of ALK (Fig. 2C). These data suggest that EGFR activation by EGF destabilized FKI binding to ROS1 and ALK.

## Proximity ligation assays reveal a novel role for EGFR as a signaling partner in fusion kinase positive lung cancer cell lines

We have shown that the fusion kinase is re-phosphorylated following EGFR activation, and that FKI binding was disrupted, but we wanted to ask whether the fusion kinase was re-engaged in signaling. We first addressed this by using phosphotyrosine-specific antibodies, and were able to identify a common phosphorylated tyrosine residue(s) mapping to the conserved activation loop of the ALK, RET, and TRKA kinases (Supplementary Fig. S3A, B). Next, based on the re-phosphorylation of tyrosines critical to kinase function, we tested whether this phosphorylation resulted in a rescue of signaling by the fusion kinase as measured by adaptor protein binding. Therefore, a proximity ligation assay (PLA) was employed to detect kinase-adaptor signaling complexes in cells (33). We designed assays to recognize complexes formed between each fusion kinase and a predicted, commonly used adaptor protein based on the conserved phosphorylated tyrosine(s) detected following inhibition and rescue with EGF (Supplementary Fig. S3A, B) (34–36). The PLA is designed to detect 2 proteins within a distance as large as 40 nanometers (33,37). We have previously shown active signaling TRK-SHC1 complexes using this approach, including the ability to disrupt these complexes by RNAi knockdown of one partner or by pharmacologic inhibition of the kinase (6). TRKA-SHC1 (CUTO-3 cells), RET-GRB7 (LC-2/ad), ROS1-GRB2



(HCC78), and ALK-GRB2 (H3122 and STE-1) kinase-adaptor PLAs revealed that each fusion was signaling through the adaptor at baseline as expected, and that these complexes were disrupted by a cognate FKI (Fig. 3A, 3C, Supplementary Fig. S3C). Importantly, the fusion kinase-adaptor signaling complexes were restored after EGF stimulation (in the presence of the FKI), and were only fully disrupted by combination treatment of the FKI and gefitinib when EGF was also present (Fig. 3A, 3C, Supplementary Fig. S3C). These data corroborate the re-phosphorylation results observed in the immunoblot experiments (Fig. 2, Supplementary Fig. S1) and support a model where EGFR signaling is not only re-phosphorylating and disrupting FKI binding, but re-engaging the signaling function of the inhibited fusion kinase.

We next queried the role of EGFR signaling in these gene fusion positive cell lines by implementing an EGFR-GRB2 PLA. This assay was validated using cell lines that demonstrate different levels of EGFR expression and activity (Supplementary Fig. S4A–C). We observed dose-dependent loss of EGFR signaling complexes in the presence of an EGFR inhibitor (Supplementary Fig. S4A, B). We observed 2 patterns of EGFR activation in the gene fusion positive cell lines: in the first type, observed in ALK and TRKA fusion cell lines, EGFR signaling complexes were present in unperturbed cells (basal EGFR activation) (Fig. 3B, 3C, Supplementary Fig. S3D). Alternatively, in ROS1 and RET fusion kinase positive cell lines, an increase in EGFR signaling complexes was observed following inhibition of the fusion kinase (induced EGFR activation) (Fig. 3B, 3C, Supplementary Fig. S3D). Thus, these assays provide additional evidence that EGFR can signal independently through GRB2 in these cells.

### Switching of adaptor proteins from fusion kinases to EGFR following FKI treatment

In order to evaluate the increase in EGFR-GRB2 signaling with FKI treatment observed in Figure 3, we performed a time course using the ROS1 cell line HCC78 and the RET cell line LC-2/ad to delineate the kinetics of the increase in EGFR-GRB2 signaling following FKI treatment. The ALK and TRK cell lines were not included, because they display higher levels of EGFR signaling prior to FKI treatment. We observed a rapid increase in EGFR signaling complexes following addition of a ROS1 inhibitor, and this was readily reversible, reverting to baseline levels upon wash out of the ROS1 inhibitor (Fig. 4A, B, D, E). This change in GRB2 adaptor binding from ROS1 to EGFR was also observed using co-immunoprecipitations following FKI treatment in the HCC78 cells (Fig. 4C). This change in binding of GRB2 from ROS1 to EGFR was specific, and did not occur with the MET RTK, which is both expressed and phosphorylated in these cells (Supplementary Fig. S5A, S5B) (13). Use of H1993 cells, which display *MET* gene amplification and are sensitive to MET inhibitors such as crizotinib, were utilized as a positive control to demonstrate that MET-GRB2 complexes could be detected using the PLA and that they were disrupted with MET inhibition (Supplementary Fig. S5C, S5D) (38). A similar result, albeit with slower kinetics, was seen in the RET+ LC-2/ad cells. Using both PLA and co-immunoprecipitation, both GRB2 and SHC1 adaptor proteins demonstrated a similar switch from RET to EGFR (Supplementary Fig. S6). Collectively, these experiments suggest that while phosphorylation is necessary to initiate signaling, it may not be a sufficient indicator of adaptor binding and the initiation of a signaling cascade. These results demonstrate the plasticity of signaling in

cancer cells as indicated by the ability of the GRB2 or SHC1 adaptors to switch from one kinase to another following short-term kinase inhibition.

### EGFR and fusion kinases can form complexes

Given the rapid phosphorylation of the fusion kinase by EGFR and the ability of GRB2 to switch to EGFR, we asked whether EGFR could exist in a complex with the fusion kinase. All 4 fusion kinases co-immunoprecipitated with EGFR both in lung cancer cells, where both proteins are endogenously expressed, and also when ectopically co-expressed in 293T cells (Supplementary Fig. 7A–H). This interaction was sustained under various kinase inhibitory and stimulatory conditions, including combined inhibition and EGF stimulation, suggesting the interaction is independent of kinase activity (Supplementary Fig. 7A–H). Overexpression of another RTK, FGFR1, did not generate complexes with ROS1, indicating a degree of specificity for the EGFR-oncogenic fusion kinase interaction (Supplementary Fig. S7I, J). Complexes between each of the fusion kinases and EGFR were also observed endogenously in each cell line using PLA (Supplementary Fig. 7K), but not with cytokeratins, another abundant class of proteins in these cells (Supplementary Fig. 7L). EGFR-fusion kinase complex detection was specific to cells harboring the correct fusion kinase, demonstrating an absence of antibody cross-reactivity (Supplementary Fig. S4M). These data provide evidence for complexes between TRKA, ALK, RET, or ROS1 fusion kinases and EGFR.

### Inhibition of EGFR enhances ALK inhibition *in vivo*

To determine the role of EGFR *in vivo*, we sought to establish whether the combination of crizotinib and gefitinib induced a more substantial reduction in tumor volume compared to monotherapy crizotinib in an ALK+ xenograft mouse model. The combination of gefitinib and crizotinib resulted in a significant decrease in tumor growth over crizotinib monotherapy (Fig. 5A). Additionally, pharmacodynamic analyses using PLA were conducted on tumors from each of the four treatment arms in this study to evaluate the target inhibition of ALK and EGFR at the termination of the study. There was a significant reduction of ALK-GRB2 and EGFR-GRB2 signaling complexes with combination therapy, compared to ALK monotherapy, consistent with the effects of combination therapy on tumor growth (Fig. 5B, C). Together, these data provide evidence for a functional role of EGFR in fusion kinase-driven cell proliferation as well as tumor maintenance.

### EGFR is expressed and activated in human lung cancers that harbor gene fusions

We next asked whether EGFR activation could be detected in a patient-derived xenograft (PDX) mouse model derived from a NSCLC patient whose tumor harbored an *NTRK1* fusion (Supplementary Fig. S8A) (1,6). Tumors from the PDX model are positive for the *NTRK1* rearrangement by FISH and demonstrate both high levels of EGFR expression and phosphorylation by immunohistochemistry (Supplementary Fig. S8B, C). FFPE tumor samples from the *NTRK1*+ PDX model were positive for TRKA-SHC1 and EGFR-GRB2 signaling complexes by PLA, as well as TRK-EGFR PLA complexes whereas an *NTRK1*-PDX model derived from a patient with an unknown oncogene was negative for each of these PLAs (Supplementary Fig. S8D–I).

EGFR is highly expressed in unselected NSCLC (24). We evaluated EGFR expression in a cohort of 26 ALK+ and ROS1+ patients who also had clinical EGFR IHC testing performed at our institution. Similar to unselected NSCLC, the majority of ALK or ROS1+ tumors had high levels of EGFR expression with 21/26 (81%) samples exhibiting an IHC score 200 (out of 300) demonstrating that EGFR is available for signaling contribution in most of these gene fusion positive tumors (Supplementary Fig. S9A).

Finally, we asked whether fusion kinase and EGFR signaling complexes could be detected in patient tumor samples. We analyzed *ROS1*, *ALK*, and *RET* positive patient tumor samples using PLAs specific for either fusion kinase-adaptor or EGFR-GRB2 complexes (Fig. 5D–E, Supplementary Fig. S9). Minimal EGFR-GRB2 signaling was detected by PLA prior to treatment with a FKI in a *ROS1*+ patient, but a significant increase in EGFR-GRB2 signaling was detected at disease progression post FKI treatment in that *ROS1*+ patient (Fig. 5D, E). Abundant levels of EGFR-GRB2 signaling complexes were also detected in resistant *ALK*+ or *RET*+ lung cancer patients (Supplementary Fig. S9). The fusion kinase-adaptor PLAs were also detected in each patient's resistant sample following or while still on treatment with an FKI. None of these tumor samples had evidence of a resistance mutation in the kinase domain to account for persistent fusion kinase activation. Thus, the persistence of fusion kinase signaling in the samples is consistent with our *in vitro* results, which demonstrated fusion kinase transactivation by EGFR (Fig. 5D, Supplementary Fig. S9B–F). A robust, distinct pattern of EGFR-GRB2 was also detected in a tumor sample from an *ALK*+ patient's brain metastasis surrounding stromal fibrovascular bundles (Supplementary Fig. S9F). The same patient samples were further tested for PLA specificity using mismatched oncogene PLAs (e.g., ALK-GRB2 PLA on RET fusion positive sample) and no PLA cross-reactivity was observed (Supplementary Fig. S9G). The *in situ* patient tumor data support the *in vitro* and *in vivo* findings, providing further evidence for a role for EGFR-GRB2 signaling in fusion kinase positive patients.

## Discussion

The work presented here demonstrates two novel mechanisms by which EGFR can rescue critical signaling in cancer cells harboring gene fusions treated with targeted inhibitors: re-activation of the drug-inhibited oncogene and dynamic adaptor protein-mediated signaling rewiring. These data suggest that wild-type EGFR, which is expressed at high levels on the majority of ALK+ human tumor samples, plays a critical role in cancer cells harboring gene fusions. While it is clear from clinical trials of crizotinib in ALK+ and ROS1+ patients that EGFR cannot sustain sufficient signaling in all patient tumors or in all cancer cells, the capability of an EGFR rescue described in this work may explain the heterogeneous or incomplete responses seen in the majority of patients (16). Notably, this work demonstrates a potential role for inhibiting wild-type EGFR using EGFR inhibitors in ALK+ or ROS1+ patients being treated with crizotinib or other ALK inhibitors, and potentially for RET+ and TRKA+ patients once targeted drugs are approved for these indications.

These studies demonstrate that EGFR can influence the activity of an oncogenic fusion kinase in cell lines derived from human tumors. Similar to the heterogeneity of responses to ALK or ROS1 inhibitors in NSCLC patients, the magnitude of EGFR contribution was also

heterogeneous, but was present in each of the 9 models tested (Supplementary Table 2) (11,12). The ability of EGFR to transactivate the fusion kinase in the absence of drug perturbation suggests that this signaling partnership with EGFR exists to augment or supplement signaling from the dominant oncogene, in this case the fusion oncogene. Incomplete attenuation of MAPK and AKT signaling by FKI alone and more complete inhibition of these pathways by FKI and EGFR inhibition support this supplementary signaling role for EGFR. Co-immunoprecipitation and PLA experiments support a model where EGFR is in a complex with the fusion kinase. Further evidence for an interaction between EGFR and the fusion kinases come from the demonstration that EGFR activation leads to phosphorylation of the fusion kinase in the presence of a potent FKI. The biotinylated drug experiments used a novel approach to demonstrate that EGFR activation leads to disruption of drug binding to the fusion kinase, further supporting a model in which EGFR is complexed with the fusion kinase. Thus, our model of oncogene addiction allows for the modulation of the dominant oncogene by other signaling nodes (Fig. 6). Recent work by several groups demonstrate that WT EGFR can positively modulate mutant *KRAS* activity and is consistent with the model in which dominant oncogenes can be modulated by non-oncogene signaling pathways (39,40).

The RTK-adaptor PLAs used in this study enabled the detection of activated EGFR signaling complexes in cell lines and FFPE sections of PDX or patient tumor samples in the absence of any detectable activating *EGFR* mutations. The rapid activation of EGFR in ROS1 and RET cell line models following fusion kinase inhibition suggest a model of dynamic signaling. In this model, cellular reprogramming, which can require days to weeks of oncogene inhibition, is not required for the cell to maintain partial signaling through critical signaling pathways despite inhibition of the dominant oncogene. Different signaling pathways (e.g., ROS1 and EGFR) are not necessarily engaged simultaneously at baseline, but a dynamic rewiring of signaling may occur following perturbations such as drug inhibition of the dominant oncogene. Adaptor proteins may demonstrate binding plasticity and “switch” from the dominant oncogene(s) to EGFR under therapeutic stress (Fig. 3B, 3C, 4A, Supplementary Fig S6). However, removal of the inhibitor allows GRB2 to revert to ROS1 binding, suggesting a preference for the dominant fusion oncogene (Fig. 4D). The interplay of adaptor binding is likely subject to many other factors, including concentration and competition in its environment, and thus may not automatically occur following phosphorylation (41). The *ROS1+* HCC78 cell line provides a strong example of cell signaling plasticity that occurs following loss of ROS1 signaling. The acute loss of ROS1 signaling after minutes of drug treatment allowed signaling via EGFR in this study (Fig. 3, and 4). Previous studies from our lab showed that ROS1 signalling suppression for several days was required for these cancer cells to adapt to signaling via an activating KIT mutation and a loss of the ROS1 fusion gene at the genomic level occurred following long term drug selection with a ROS1 inhibitor, permitting a switch to WT EGFR dependence (13,42). Our adaptive signaling model is supported by recent work using phosphoproteomic approaches, which demonstrated that GRB2 was bound to EGFR in unperturbed ALK+ lung cancer cells and that EGFR phosphorylation increased in response to crizotinib treatment (43). Collectively, these data demonstrate a need for the loss of the oncogene to occur in order to

allow signaling re-wiring. These data support an approach of targeting the fusion kinase and EGFR at the initiation of therapy in order to prevent this re-wiring (Fig. 6).

Growth factor ligands have previously been shown to mediate resistance to targeted inhibition of dominant oncogenes in various cell types by activating by-pass signaling pathways (13,27,44,45). Importantly, EGF and other EGFR ligands can signal in an autocrine, paracrine, or juxtacrine manner and they are expressed or upregulated in lung cancer (13,45,46). Prior studies demonstrated a mechanism whereby ligand engagement leads to bypass of the dominant oncogene. This indirect rescue of downstream signaling by the EGF/EGFR axis (Fig. 1A, 1C, Supplementary Fig. S1) in this study is consistent with prior studies demonstrating this in ALK and ROS1+ cells (45); however, extend these findings to RET and TRKA human-derived cancer cell models, suggesting that this is a common feature amongst fusion oncogene-driven cancer cells. As described above, our data suggest additional mechanisms by which growth factor ligands can mediate resistance to oncogene-targeted therapy (Fig. 6).

Other studies have shown a role for EGFR or other ERBB family members in mediating *acquired* resistance in ALK+ and ROS1+ cell lines (13,47–50). The common dependence of EGFR and the ERBB family for acquired resistance likely reflect the critical role and intrinsic wiring towards EGFR in cells harboring oncogene fusions prior to treatment with oncogene-directed therapy. Our studies do not rule out a potential role of other HER family members such as HER2 or HER3 as these RTKs are known to heterodimerize with EGFR or signal independently. However, gefitinib is far less potent against HER2 than EGFR and we used a dose of gefitinib that discriminates between these RTKs (51). Also, EGFR is a more attractive target as it is more widely expressed than HER2 in NSCLC patients (24,52). We speculate that cells are likely to rely on pre-existing signaling pathways for acquired resistance, rather than generating bypass signaling de novo from signaling programs that do not pre-exist. Although additional models will need to be identified and tested, our observations in a colorectal cancer cell line KM12 harboring the *TPM3-NTRK1* fusion suggests that this role for EGFR in the context of fusion kinases might also apply to malignancies other than lung cancer (9,53,54). Previous work in other cancers demonstrating similar cross talk between RTKs and oncogenes phenotypes may indicate additional relevance to our studies in other cancers (55–57).

Two clinical trials of an ALK inhibitor plus an EGFR inhibitor have been conducted. Both studies utilized crizotinib as a MET inhibitor with the intent of treating MET-driven acquired resistance in patients with EGFR mutant lung cancer. A phase I study of erlotinib plus crizotinib was conducted, however the ALK and ROS1 status were not collected in this trial to determine whether there was any activity in this population (58). A phase I trial of dacomitinib plus crizotinib was also conducted, but none of the patients were positive for an ALK rearrangement (59). Both studies required dose reduction of crizotinib, thus highlighting the potential for increased toxicities with combinations of TKIs and the need for alternative strategies for inhibiting wild-type EGFR and this work is currently ongoing in our laboratory.

In summary, these studies identify a significant contribution by EGFR signaling to the oncogenic program of four different fusion kinases and demonstrate that EGFR can enable an early, adaptive rescue of signaling in cancer cells whose dominant oncogenes are inhibited. Importantly, exogenous EGF is not necessary for all of the EGFR roles described here in maintaining critical signaling in cancer cells. Notably, all of the EGFR contributions could be abrogated with the EGFR TKI gefitinib. Ongoing work will determine other potential pharmacologic strategies to inhibit WT EGFR in the clinic. Further investigation of inhibition of EGFR in combination with oncogene-specific inhibitors is warranted to determine if these combinations will deepen and/or prolong initial patient responses, and perhaps ultimately delay the onset of disease progression by acquired resistance.

## Supplementary Material

Refer to Web version on PubMed Central for supplementary material.

## Acknowledgments

The authors sincerely thank Adriana Estrada-Bernal, Chad G. Pearson, Ricardo Pineda, Harshani R. Lawrence, and Barbara A. Helfrich for their assistance with the studies pertaining to this manuscript. We also thank Pasi A. Jänne from the Dana Farber Cancer Institute and Christine M. Lovly from Vanderbilt-Ingram Cancer Center for providing cell lines used in this study. We also would like to thank also thank GlaxoSmithKline and Array Biopharma for providing foretinib (XL-880) and ARRY-470, respectively. We would also like to thank Patrick Chestnut and the Molecular Pathology Shared Resource for their assistance with collection of patient specimens for these studies.

### Financial Support

This publication was supported by the NIH/NCI 1 R01 CA193935, V Foundation for Cancer Research, NIH/NCI P50 CA058187 (University of Colorado Lung Cancer SPORE, P.A. Bunn PI), NIH/NCI 5 K12 CA086913 to R.C. Doebele; NIH/NCATS UL1 TR000154 (Colorado CTSI, R.J. Sokol PI) to L. Schubert; NIH/NCI 1 R01 CA181746 to U. Rix; NIH/NCI R21 CA181848 and Florida Biomedical Research Program 5BC07 to E.B. Haura; and NIH/NCI P30-CA076292 Cancer Center Support Grant to the H. Lee Moffitt Cancer Center Core Facilities.

## References

1. Vaishnavi A, Capelletti M, Le AT, Kako S, Butaney M, Ercan D, et al. Oncogenic and drug-sensitive NTRK1 rearrangements in lung cancer. *Nature medicine*. 2013; 19:1469–72.
2. Takeuchi K, Soda M, Togashi Y, Suzuki R, Sakata S, Hatano S, et al. RET, ROS1 and ALK fusions in lung cancer. *Nature medicine*. 2012; 18:378–81.
3. Weinstein IB. Cancer. Addiction to oncogenes—the Achilles heel of cancer. *Science*. 2002; 297:63–4. [PubMed: 12098689]
4. Shaw AT, Kim DW, Nakagawa K, Seto T, Crino L, Ahn MJ, et al. Crizotinib versus chemotherapy in advanced ALK-positive lung cancer. *N Engl J Med*. 2013; 368:2385–94. [PubMed: 23724913]
5. Shaw AT, Ou SH, Bang YJ, Camidge DR, Solomon BJ, Salgia R, et al. Crizotinib in ROS1-Rearranged Non-Small-Cell Lung Cancer. *N Engl J Med*. 2014
6. Doebele RC, Davis LE, Vaishnavi A, Le AT, Estrada-Bernal A, Keysar S, et al. An Oncogenic NTRK Fusion in a Patient with Soft-Tissue Sarcoma with Response to the Tropomyosin-Related Kinase Inhibitor LOXO-101. *Cancer Discov*. 2015; 5:1049–57. [PubMed: 26216294]
7. Drilon A, Wang L, Hasanovic A, Suehara Y, Lipson D, Stephens P, et al. Response to Cabozantinib in patients with RET fusion-positive lung adenocarcinomas. *Cancer Discov*. 2013; 3:630–5. [PubMed: 23533264]
8. Drilon A, Rekhtman N, Arcila M, Wang L, Ni A, Albano M, et al. Cabozantinib in patients with advanced RET-rearranged non-small-cell lung cancer: an open-label, single-centre, phase 2, single-arm trial. *Lancet Oncol*. 2016

9. Kumar-Sinha C, Kalyana-Sundaram S, Chinnaiyan AM. Landscape of gene fusions in epithelial cancers: seq and ye shall find. *Genome Med.* 2015; 7:129. [PubMed: 26684754]
10. Shaw AT, Hsu PP, Awad MM, Engelman JA. Tyrosine kinase gene rearrangements in epithelial malignancies. *Nature reviews Cancer.* 2013; 13:772–87. [PubMed: 24132104]
11. Solomon BJ, Mok T, Kim DW, Wu YL, Nakagawa K, Mekhail T, et al. First-line crizotinib versus chemotherapy in ALK-positive lung cancer. *N Engl J Med.* 2014; 371:2167–77. [PubMed: 25470694]
12. Shaw AT, Ou SH, Bang YJ, Camidge DR, Solomon BJ, Salgia R, et al. Crizotinib in ROS1-rearranged non-small-cell lung cancer. *N Engl J Med.* 2014; 371:1963–71. [PubMed: 25264305]
13. Davies KD, Mahale S, Astling DP, Aisner DL, Le AT, Hinz TK, et al. Resistance to ROS1 inhibition mediated by EGFR pathway activation in non-small cell lung cancer. *PLoS one.* 2013; 8:e82236. [PubMed: 24349229]
14. Katayama R, Khan TM, Benes C, Lifshits E, Ebi H, Rivera VM, et al. Therapeutic strategies to overcome crizotinib resistance in non-small cell lung cancers harboring the fusion oncogene EML4-ALK. *Proc Natl Acad Sci U S A.* 2011; 108:7535–40. [PubMed: 21502504]
15. Doebele RC, Pilling AB, Aisner DL, Kutateladze TG, Le AT, Weickhardt AJ, et al. Mechanisms of resistance to crizotinib in patients with ALK gene rearranged non-small cell lung cancer. *Clinical cancer research : an official journal of the American Association for Cancer Research.* 2012; 18:1472–82. [PubMed: 22235099]
16. Bivona TG, Doebele RC. A framework for understanding and targeting residual disease in oncogene-driven solid cancers. *Nat Med.* 2016; 22:472–8. [PubMed: 27149220]
17. Kazandjian, DGB,GM., Zhang, L., McCoach, CE., Tang, S., Sridhara, R., Doebele, RC., Keegan, P., Pazdur, R. *J Clin Oncol.* Chicago, IL: 2016. Exploratory responder analyses of greatest depth of response (DepOR) and survival in patients with metastatic non-small cell lung cancer (mNSCLC) treated with treated with a targeted therapy or immunotherapy.
18. Pazarentzos E, Bivona TG. Adaptive stress signaling in targeted cancer therapy resistance. *Oncogene.* 2015; 34:5599–606. [PubMed: 25703329]
19. Hata AN, Niederst MJ, Archibald HL, Gomez-Carballo M, Siddiqui FM, Mulvey HE, et al. Tumor cells can follow distinct evolutionary paths to become resistant to epidermal growth factor receptor inhibition. *Nat Med.* 2016
20. Holbro T, Hynes NE. ErbB receptors: directing key signaling networks throughout life. *Annu Rev Pharmacol Toxicol.* 2004; 44:195–217. [PubMed: 14744244]
21. Bonner JA, Harari PM, Giralt J, Azarnia N, Shin DM, Cohen RB, et al. Radiotherapy plus cetuximab for squamous-cell carcinoma of the head and neck. *N Engl J Med.* 2006; 354:567–78. [PubMed: 16467544]
22. Van Cutsem E, Kohne CH, Hitre E, Zaluski J, Chang Chien CR, Makhson A, et al. Cetuximab and chemotherapy as initial treatment for metastatic colorectal cancer. *N Engl J Med.* 2009; 360:1408–17. [PubMed: 19339720]
23. Thatcher N, Hirsch FR, Luft AV, Szczesna A, Ciuleanu TE, Dediu M, et al. Necitumumab plus gemcitabine and cisplatin versus gemcitabine and cisplatin alone as first-line therapy in patients with stage IV squamous non-small-cell lung cancer (SQUIRE): an open-label, randomised, controlled phase 3 trial. *Lancet Oncol.* 2015; 16:763–74. [PubMed: 26045340]
24. Rusch V, Baselga J, Cordon-Cardo C, Orazem J, Zaman M, Hoda S, et al. Differential expression of the epidermal growth factor receptor and its ligands in primary non-small cell lung cancers and adjacent benign lung. *Cancer Res.* 1993; 53:2379–85. [PubMed: 7683573]
25. Helfrich BA, Raben D, Varella-Garcia M, Gustafson D, Chan DC, Bemis L, et al. Antitumor activity of the epidermal growth factor receptor (EGFR) tyrosine kinase inhibitor gefitinib (ZD1839, Iressa) in non-small cell lung cancer cell lines correlates with gene copy number and EGFR mutations but not EGFR protein levels. *Clin Cancer Res.* 2006; 12:7117–25. [PubMed: 17145836]
26. Koivunen JP, Mermel C, Zejnullahu K, Murphy C, Lifshits E, Holmes AJ, et al. EML4-ALK fusion gene and efficacy of an ALK kinase inhibitor in lung cancer. *Clinical cancer research : an official journal of the American Association for Cancer Research.* 2008; 14:4275–83. [PubMed: 18594010]

27. Lovly CM, McDonald NT, Chen H, Ortiz-Cuaran S, Heukamp LC, Yan Y, et al. Rationale for co-targeting IGF-1R and ALK in ALK fusion-positive lung cancer. *Nat Med.* 2014; 20:1027–34. [PubMed: 25173427]
28. Davies KD, Le AT, Theodoro MF, Skokan MC, Aisner DL, Berge EM, et al. Identifying and targeting ROS1 gene fusions in non-small cell lung cancer. *Clin Cancer Res.* 2012; 18:4570–9. [PubMed: 22919003]
29. Carpenter AE, Jones TR, Lamprecht MR, Clarke C, Kang IH, Friman O, et al. CellProfiler: image analysis software for identifying and quantifying cell phenotypes. *Genome Biol.* 2006; 7:R100. [PubMed: 17076895]
30. Hirsch FR, Varella-Garcia M, Bunn PA Jr, Di Maria MV, Veve R, Bremmes RM, et al. Epidermal growth factor receptor in non-small-cell lung carcinomas: correlation between gene copy number and protein expression and impact on prognosis. *Journal of clinical oncology : official journal of the American Society of Clinical Oncology.* 2003; 21:3798–807. [PubMed: 12953099]
31. Keysar SB, Astling DP, Anderson RT, Vogler BW, Bowles DW, Morton JJ, et al. A patient tumor transplant model of squamous cell cancer identifies PI3K inhibitors as candidate therapeutics in defined molecular bins. *Mol Oncol.* 2013; 7:776–90. [PubMed: 23607916]
32. Rix U, Superti-Furga G. Target profiling of small molecules by chemical proteomics. *Nat Chem Biol.* 2009; 5:616–24. [PubMed: 19690537]
33. Smith MA, Hall R, Fisher K, Haake SM, Khalil F, Schabath MB, et al. Annotation of human cancers with EGFR signaling-associated protein complexes using proximity ligation assays. *Science signaling.* 2015; 8:ra4. [PubMed: 25587191]
34. Hallberg B, Palmer RH. Mechanistic insight into ALK receptor tyrosine kinase in human cancer biology. *Nature reviews Cancer.* 2013; 13:685–700. [PubMed: 24060861]
35. Pandey A, Liu X, Dixon JE, Di Fiore PP, Dixit VM. Direct association between the Ret receptor tyrosine kinase and the Src homology 2-containing adapter protein Grb7. *The Journal of biological chemistry.* 1996; 271:10607–10. [PubMed: 8631863]
36. Stephens RM, Loeb DM, Copeland TD, Pawson T, Greene LA, Kaplan DR. Trk receptors use redundant signal transduction pathways involving SHC and PLC-gamma 1 to mediate NGF responses. *Neuron.* 1994; 12:691–705. [PubMed: 8155326]
37. Soderberg O, Gullberg M, Jarvius M, Ridderstrale K, Leuchowius KJ, Jarvius J, et al. Direct observation of individual endogenous protein complexes in situ by proximity ligation. *Nat Methods.* 2006; 3:995–1000. [PubMed: 17072308]
38. Tanizaki J, Okamoto I, Okamoto K, Takezawa K, Kuwata K, Yamaguchi H, et al. MET tyrosine kinase inhibitor crizotinib (PF-02341066) shows differential antitumor effects in non-small cell lung cancer according to MET alterations. *J Thorac Oncol.* 2011; 6:1624–31. [PubMed: 21716144]
39. Umelo IA, De Wever O, Kronenberger P, Van Deun J, Noor A, Singh K, et al. Combined targeting of EGFR/HER promotes anti-tumor efficacy in subsets of KRAS mutant lung cancer resistant to single EGFR blockade. *Oncotarget.* 2015; 6:20132–44. [PubMed: 25992771]
40. Lito P, Solomon M, Li LS, Hansen R, Rosen N. Allele-specific inhibitors inactivate mutant KRAS G12C by a trapping mechanism. *Science.* 2016; 351:604–8. [PubMed: 26841430]
41. Crowe DL, Tsang KJ. Decreased mitogenic response to epidermal growth factor in human squamous cell carcinoma lines overexpressing epidermal growth factor receptor owing to limiting amounts of the adaptor protein Grb2: rescue by retinoic acid treatment. *Mol Carcinog.* 2001; 32:187–94. [PubMed: 11746830]
42. Dziadziuszko R, Le AT, Wrona A, Jassem J, Camidge DR, Varella-Garcia M, et al. An Activating KIT Mutation Induces Crizotinib Resistance in ROS1-Positive Lung Cancer. *J Thorac Oncol.* 2016; 11:1273–81. [PubMed: 27068398]
43. Zhang G, Scarborough H, Kim J, Rozhok AI, Chen YA, Zhang X, et al. Coupling an EML4-ALK-centric interactome with RNA interference identifies sensitizers to ALK inhibitors. *Sci Signal.* 2016; 9:rs12. [PubMed: 27811184]
44. Tanimoto A, Yamada T, Nanjo S, Takeuchi S, Ebi H, Kita K, et al. Receptor ligand-triggered resistance to alectinib and its circumvention by Hsp90 inhibition in EML4-ALK lung cancer cells. *Oncotarget.* 2014



45. Wilson TR, Fridlyand J, Yan Y, Penuel E, Burton L, Chan E, et al. Widespread potential for growth-factor-driven resistance to anticancer kinase inhibitors. *Nature*. 2012; 487:505–9. [PubMed: 22763448]
46. Obenauf AC, Zou Y, Ji AL, Vanharanta S, Shu W, Shi H, et al. Therapy-induced tumour secretomes promote resistance and tumour progression. *Nature*. 2015; 520:368–72. [PubMed: 25807485]
47. Sasaki T, Koivunen J, Ogino A, Yanagita M, Nikiforow S, Zheng W, et al. A novel ALK secondary mutation and EGFR signaling cause resistance to ALK kinase inhibitors. *Cancer Res*. 2011; 71:6051–60. [PubMed: 21791641]
48. Voena C, Di Giacomo F, Panizza E, D'Amico L, Boccalatte FE, Pellegrino E, et al. The EGFR family members sustain the neoplastic phenotype of ALK+ lung adenocarcinoma via EGR1. *Oncogenesis*. 2013; 2:e43. [PubMed: 23567620]
49. Tani T, Yasuda H, Hamamoto J, Kuroda A, Arai D, Ishioka K, et al. Activation of EGFR Bypass Signaling by TGF $\alpha$  Overexpression Induces Acquired Resistance to Alectinib in ALK-Translocated Lung Cancer Cells. *Molecular cancer therapeutics*. 2016; 15:162–71. [PubMed: 26682573]
50. Dong X, Fernandez-Salas E, Li E, Wang S. Elucidation of Resistance Mechanisms to Second-Generation ALK Inhibitors Alectinib and Ceritinib in Non-Small Cell Lung Cancer Cells. *Neoplasia*. 2016; 18:162–71. [PubMed: 26992917]
51. Karaman MW, Herrgard S, Treiber DK, Gallant P, Atteridge CE, Campbell BT, et al. A quantitative analysis of kinase inhibitor selectivity. *Nat Biotechnol*. 2008; 26:127–32. [PubMed: 18183025]
52. Takenaka M, Hanagiri T, Shinohara S, Kuwata T, Chikaishi Y, Oka S, et al. The prognostic significance of HER2 overexpression in non-small cell lung cancer. *Anticancer Res*. 2011; 31:4631–6. [PubMed: 22199341]
53. Lovly CM, Gupta A, Lipson D, Otto G, Brennan T, Chung CT, et al. Inflammatory Myofibroblastic Tumors harbor multiple potentially actionable kinase fusions. *Cancer Discov*. 2014
54. Le AT, Doebele RC. The democratization of the oncogene. *Cancer Discov*. 2014; 4:870–2. [PubMed: 25092743]
55. Javidi-Sharifi N, Traer E, Martinez J, Gupta A, Taguchi T, Dunlap J, et al. Crosstalk between KIT and FGFR3 Promotes Gastrointestinal Stromal Tumor Cell Growth and Drug Resistance. *Cancer Res*. 2015; 75:880–91. [PubMed: 25432174]
56. Croyle M, Akeno N, Knauf JA, Fabbro D, Chen X, Baumgartner JE, et al. RET/PTC-induced cell growth is mediated in part by epidermal growth factor receptor (EGFR) activation: evidence for molecular and functional interactions between RET and EGFR. *Cancer Res*. 2008; 68:4183–91. [PubMed: 18519677]
57. Morrison KB, Tognon CE, Garnett MJ, Deal C, Sorensen PH. ETV6-NTRK3 transformation requires insulin-like growth factor 1 receptor signaling and is associated with constitutive IRS-1 tyrosine phosphorylation. *Oncogene*. 2002; 21:5684–95. [PubMed: 12173038]
58. Ou SI, Govindan R, Eaton KD, Otterson GA, Gutierrez ME, Mita AC, et al. Phase I Results from a Study of Crizotinib in Combination with Erlotinib in Patients with Advanced Nonsquamous Non-Small Cell Lung Cancer. *J Thorac Oncol*. 2017; 12:145–51. [PubMed: 27697581]
59. Janne PA, Shaw AT, Camidge DR, Giaccone G, Shreeve SM, Tang Y, et al. Combined Pan-HER and ALK/ROS1/MET Inhibition with Dacomitinib and Crizotinib in Advanced Non-Small Cell Lung Cancer: Results of a Phase I Study. *J Thorac Oncol*. 2016; 11:737–47. [PubMed: 26899759]

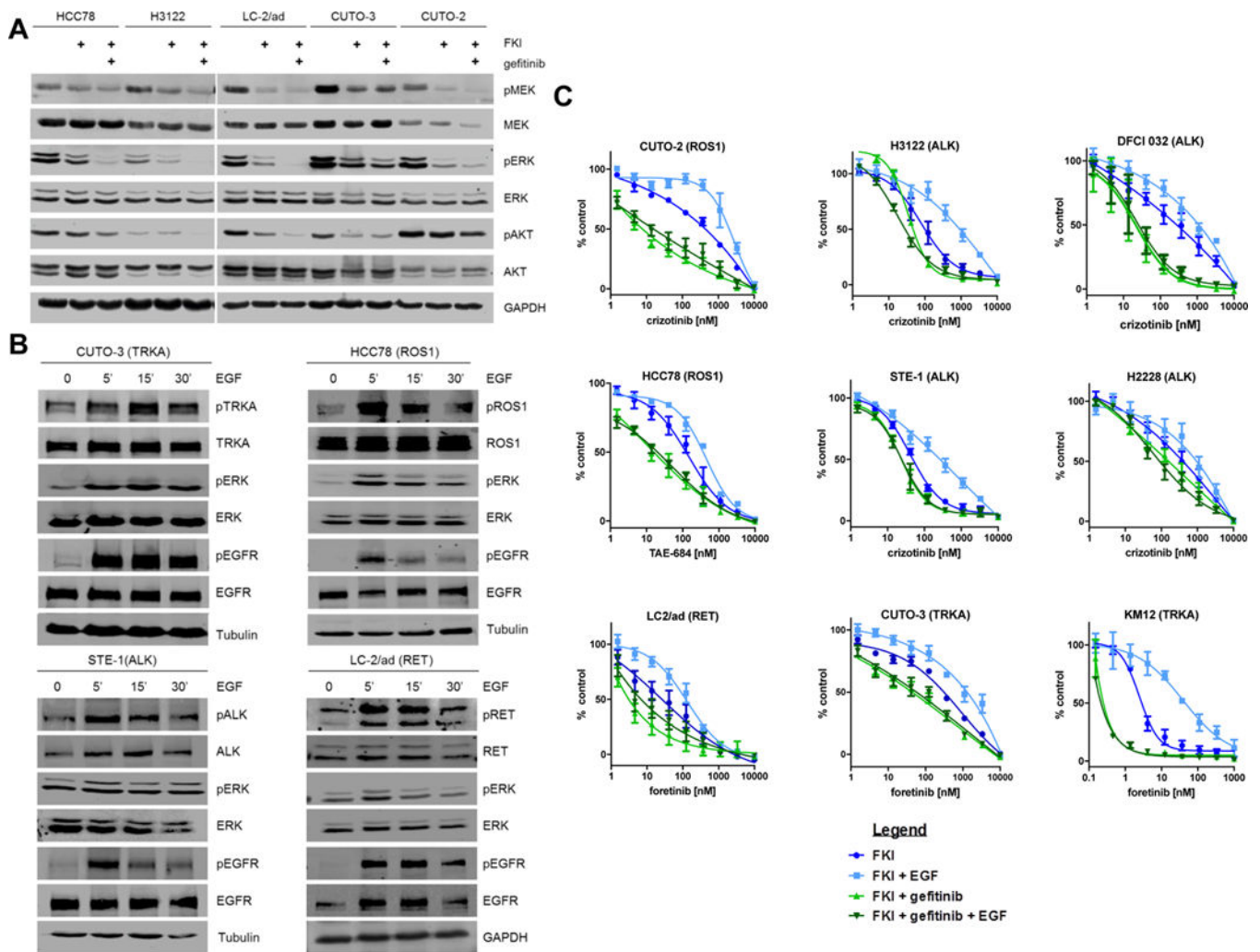


**Figure 1. EGFR blockade improves inhibition of downstream signaling, proliferation, and EGF stimulation increases unperturbed fusion kinase phosphorylation and proliferation**

**A**, NSCLC fusion kinase positive cell lines HCC78 (ROS1), H3122 (ALK), LC-2/ad (RET), CUTO-3 (TRKA), and CUTO-2 (ROS1) were treated with either a vehicle control, cognate fusion kinase inhibitor: 250 nM TAE-684 (HCC78 ROS1), 250 nM crizotinib (ALK or ROS1), 250 nM foretinib (RET), or 100nM ARRY-470 (TRKA), or FKI with 1  $\mu$ M gefitinib. Downstream signaling changes were evaluated with pMEK1/2 (S217/221), S473 for pAKT, T202 and Y202 for pERK.  $n = 3$ . **B**, Immunoblot analysis of CUTO-3 cells phosphorylation kinetics for EGFR, RIP-TRKA, and ERK following vehicle control (PBS) stimulation, 5, 15, and 30 minutes of 100 ng/mL EGF stimulation. Blots were probed with Y1068 and Y1173 or 4G10 for pEGFR, Y496 and Y680/681 for pTRKA, and T202 and Y204 for pERK. Representative images of blots are shown. Identical immunoblot analysis of HCC78 cells (ROS1) STE-1 cells (ALK) and LC-2/ad (RET) cells for pEGFR, the corresponding fusion kinase phosphorylation, and pERK following the indicated time course of 100 ng/mL EGF stimulation (5, 15, and 30 minutes.)  $n = 3$ . **C**, Cell lines that harbor gene fusions were treated with the indicated FKI alone (dark blue dose curve, x-axis), FKI + 1  $\mu$ M gefitinib (green), or FKI + 100 ng/mL EGF (light blue) for 72 hours and assessed using MTS. Each condition

was performed in experimental triplicate, data are expressed as the mean  $\pm$  the SEM. IC<sub>50</sub> values and statistical analysis for each condition are shown in Supplementary Table 1. Biological repeats of all 9 cell lines were pooled for statistical analysis.

Author Manuscript

Author Manuscript

Author Manuscript

Author Manuscript

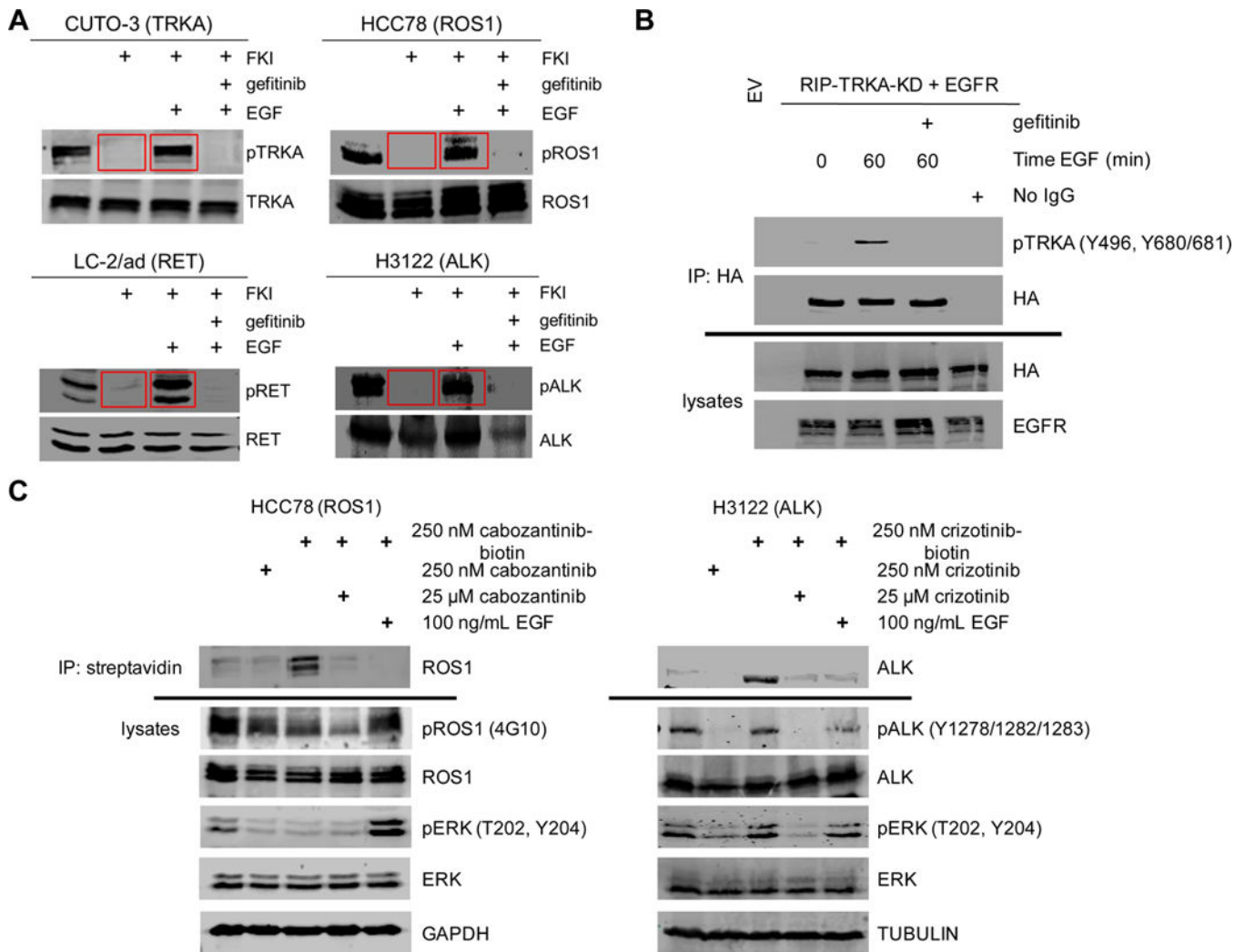


**Figure 2. EGFR re-activates targeted inhibition or an inactive state of TRKA, RET, ROS1, and ALK fusion kinase domains**

**A**, NSCLC fusion kinase positive cell lines CUTO-3, LC-2/ad, HCC78 cells, and H3122 cells were treated for 3 hours with vehicle control (DMSO), a cognate fusion kinase inhibitor: 100nM ARRY-470 (TRKA), 250 nM foretinib (RET), 500 nM TAE-684 (ROS1), or 250 nM crizotinib (ALK), 1 μM gefitinib, or the combination of FKI and gefitinib, in the absence or presence of 30 minutes of 100ng/mL EGF stimulation. Red boxes highlight rescued fusion phosphorylation with the addition of EGF in the presence of the FKI. Immunoblot analysis was performed using the antibodies indicated. Phospho-specific antibodies to Y496 Y680/681 were used for pTRKA, and 4G10 was used for pROS1, pRET, and pALK as shown. A more comprehensive evaluation of the signaling changes under each treatment condition is shown in fig. S1.  $n = 3$ . **B**, EGFR and HA-tagged catalytically inactive RIP-TRKA (K544N) or an empty-PCDH vector cDNA were transiently expressed in 293T cells for 24 hours and treated with DMSO vehicle, stimulated with 100 ng/mL EGF for 60 minutes, or with 1 μM gefitinib for 2 hours, and immunoprecipitated with the HA antibody, and immunoblotted for phospho-TRKA at Y496, and Y680/481 or HA. Immunoblotted lysates from the same experiment are shown.  $n = 3$ . **C**, Immunoblot analysis of HCC78 or

H3122 cell lysates treated with vehicle control (DMSO), 250 nM cabozantinib or crizotinib, 250 nM of biotin conjugated cabozantinib or biotin conjugated crizotinib, in the presence of 100× unconjugated crizotinib, or 100 ng/mL EGF and immunoprecipitated with streptavidin conjugated magnetic beads. Blots were then probed for total ROS1 or ALK to assess the ability of cabozantinib or crizotinib to bind specifically to ROS1 or ALK, under the inhibitor only and inhibitor plus EGF stimulated conditions. Lysates were also probed for downstream pERK to indicate similar potency and no interference of the linker of biotinylated crizotinib compared to unlabeled crizotinib.

Author Manuscript

Author Manuscript

Author Manuscript

Author Manuscript

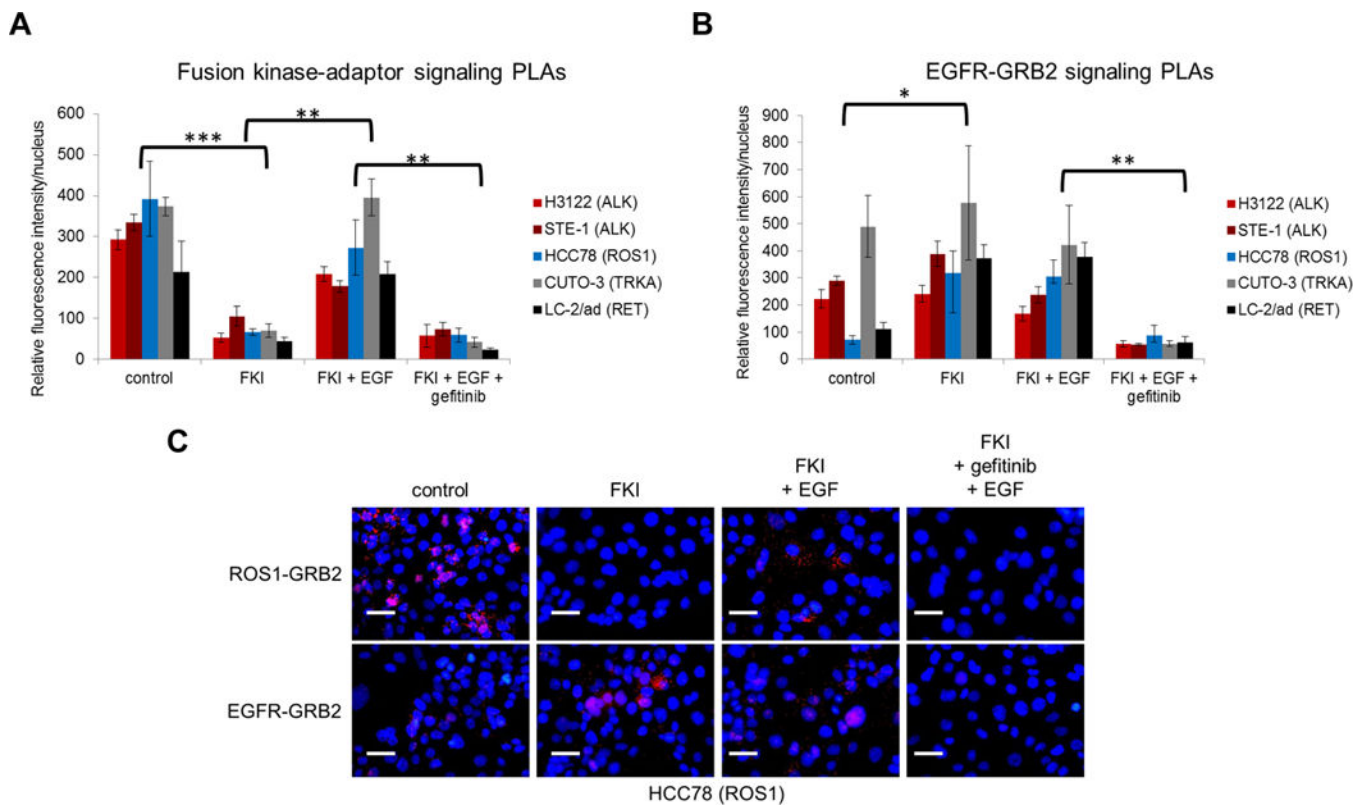


**Figure 3. EGFR restores pharmacological disruption of conserved fusion kinase tyrosines, disruption of signaling complexes, and signals independently through GRB2 in fusion kinase NSCLC cell lines**

**A**, Quantification of fusion kinase-adaptor PLAs in the indicated cell lines: TRKA-SHC1 (CUTO-3; FKI = 250 nM foretinib), RET-GRB7 (LC-2/ad; FKI = 250 nM foretinib), ROS1-GRB2 (HCC78; FKI=200 nM TAE-684), and ALK-GRB2 (H3122; FKI=250 nM crizotinib; STE-1; FKI=250 nM crizotinib) were treated with DMSO, FKI, FKI + 20 minute stimulation with 100 ng/ML EGF, or FKI + 1  $\mu$ m gefitinib + EGF.  $n = 3$ . PLAs were quantified using CellProfiler software to demonstrate significance of qualitative changes of the red fluorescent signal averaged across at least a total of 250 nuclei per experiments. Statistical analysis was performed across average fold changes in red fluorescence intensity averaged across all 5 cell lines.  $P$  values were calculated using a paired student's  $t$  test. \* indicates  $p < 0.05$ , \*\*  $p < 0.01$ , \*\*\*  $p < 0.005$ . **B**, Quantification of the EGFR-GRB2 PLAs in the indicated cell lines, with the same drug treatment conditions as described in **A**.  $n = 3$ . Statistical analysis was performed across average changes in red fluorescence intensity across all 5 cell lines.  $P$  values were calculated using a paired student's  $t$  test. \* indicates  $p < 0.05$ , \*\*  $p < 0.01$ . Data in both **A**, and **B**, is expressed as the mean  $\pm$  the SEM. **C**, Representative images from experiments in **A**, and **B**, are shown for the HCC78 (ROS1) cell line under the 4 treatment conditions. Scale bars shown represent approximately 50 microns.

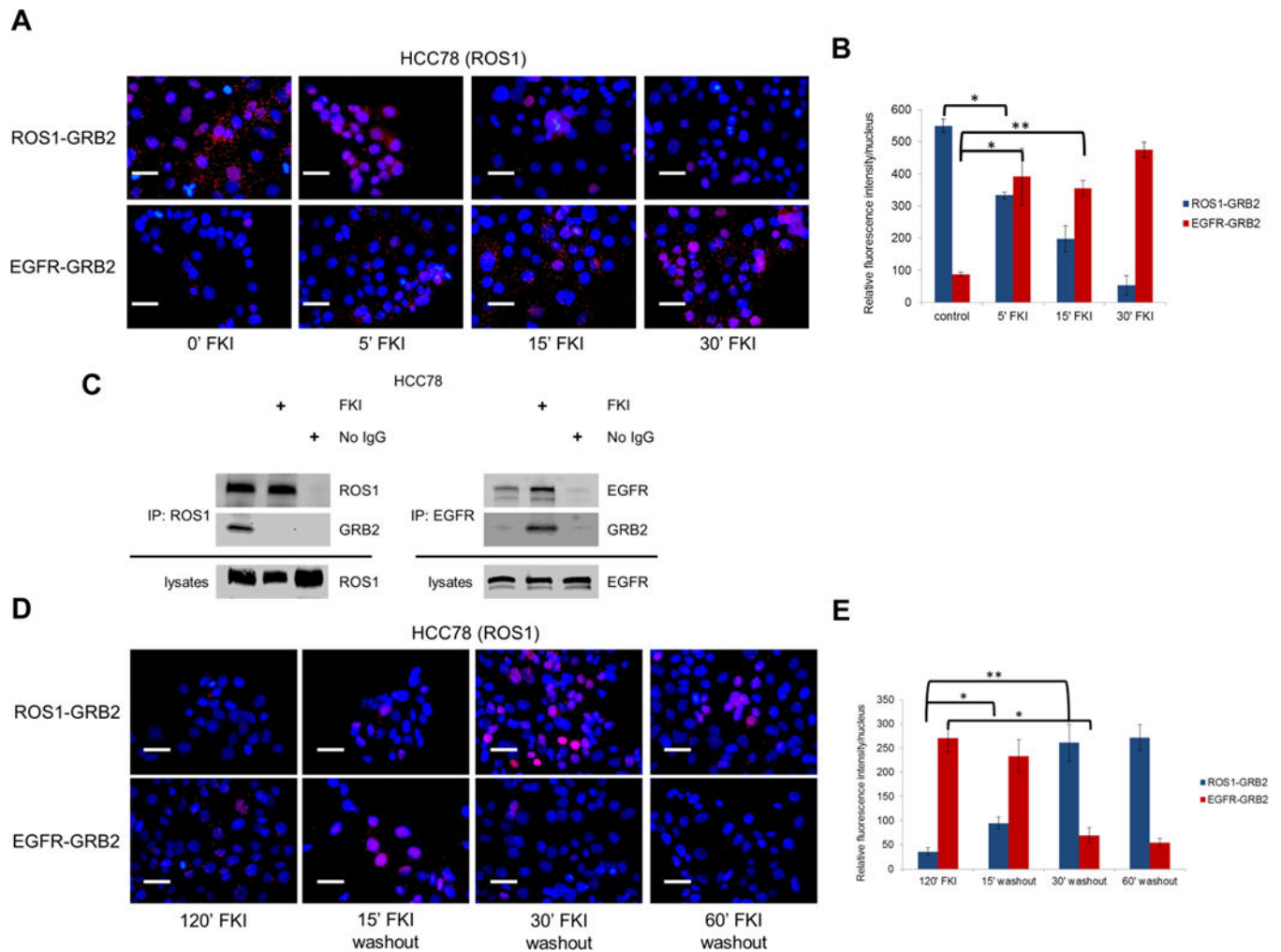


**Figure 4. Timecourse of GRB2 signaling in a ROS1+ cell line treated with a fusion kinase inhibitor (FKI) reveals the changes are rapid and reversible**

**A**, Time course of FKI treatment in HCC78 *ROS1*+ cells fixed at the indicated timepoints, and assayed by ROS1-GRB2 or EGFR-GRB2 PLAs. FKI= 250 nM TAE-684.

Representative images are shown.  $n = 3$ . **B**, Quantification of experiments described in **A**.

Data is expressed as the mean  $\pm$  the SEM.  $P$  values were calculated using a paired student's  $t$

test \* indicates  $p < 0.05$ , \*\*  $p < 0.01$ , \*\*\*  $p < 0.005$ . **C**, ROS1 or EGFR was

immunoprecipitated from HCC78 parental cells followed by immunoblot analysis using

anti- ROS1, EGFR, or GRB2 antibodies after treatment with vehicle (DMSO) or FKI; 250

nM TAE-684 for 2 hours. **D**, After two hours of FKI treatment, cells were washed twice in

PBS and maintained in fresh media at the designated "washout" time until fixation. Cells

were assayed by ROS1-GRB2 or EGFR-GRB2 PLA accordingly. Representative images are

shown.  $n = 3$ . **E**, Quantification of experiments described in **A**. Data is expressed as the

mean  $\pm$  the SEM. \* indicates  $p < 0.05$ , \*\*  $p < 0.01$ . Scale bars shown represent

approximately 50 microns.

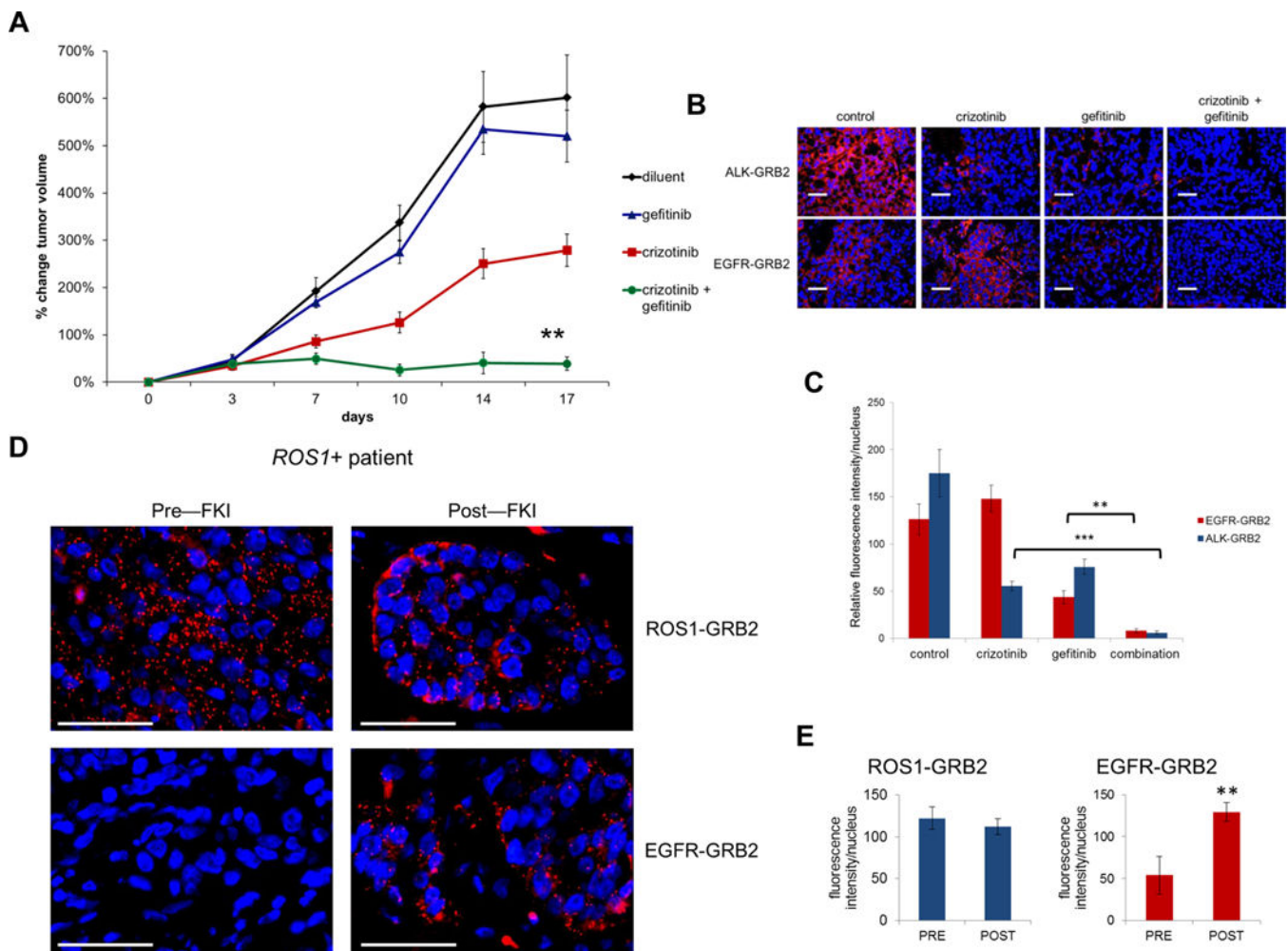


**Figure 5. EGFR contributes to the oncogenic program in fusion kinase driven lung cancer *in vivo*, and EGFR signaling complexes are present in *ROS1*+ and *ALK*+ patient samples resistant to crizotinib**

**A**, Graph depicting changes in tumor volume in an H3122 xenograft mouse model over the course of 17 days of treatment with vehicle (black), gefitinib (blue), crizotinib (red), or the combination (green) of crizotinib and gefitinib. Each treatment group started with 20 tumors at approximately 250 mm<sup>3</sup> at study baseline. Statistical analysis was performed using Bonferroni's multiple comparison ANOVA test: crizotinib vs. control,  $p < 0.05$ ; crizotinib vs. gefitinib,  $p < 0.001$ ; gefitinib vs. control, not significant; crizotinib + gefitinib vs. control,  $p < 0.001$ ; crizotinib + gefitinib vs. gefitinib,  $p < 0.001$ ; and crizotinib vs. crizotinib + gefitinib,  $p < 0.05$  ( $n = 20$  tumors per group, except control  $n = 19$ ). **B**, 5 FFPE tumors from each of the 4 treatment groups were blindly analyzed by ALK-GRB2 or EGFR-GRB2 PLA signaling analysis for a pharmacodynamics assessment of the effects of the drugs on the indicated signaling pathways in each mouse tumor. Representative images from each group are shown. Scale bars shown represent approximately 50 microns. **C**, Quantification of all ALK-GRB2 and EGFR-GRB2 PLAs across tumors from each treatment group. Data is expressed as the mean  $\pm$  the SEM. All  $P$  values were calculated using a paired student's  $t$  test. \* indicates  $p < 0.05$ , \*\*  $p < 0.01$ . **D**, FFPE tumor samples from a *ROS1*+ patient pre-



and post-treatment (at disease progression) with the FKI crizotinib were analyzed using ROS1-GRB2 and EGFR-GRB2 PLA. **E**, Quantification of PLA signal for both ROS1-GRB2 and EGFR-GRB2 signaling complexes is shown. Data is expressed as the mean  $\pm$  the SEM. *P* values were calculated using a paired student's t-test. \*\*  $p < 0.01$  Representative images are shown in both **B** and **D**. Scale bars shown represent approximately 50 microns.

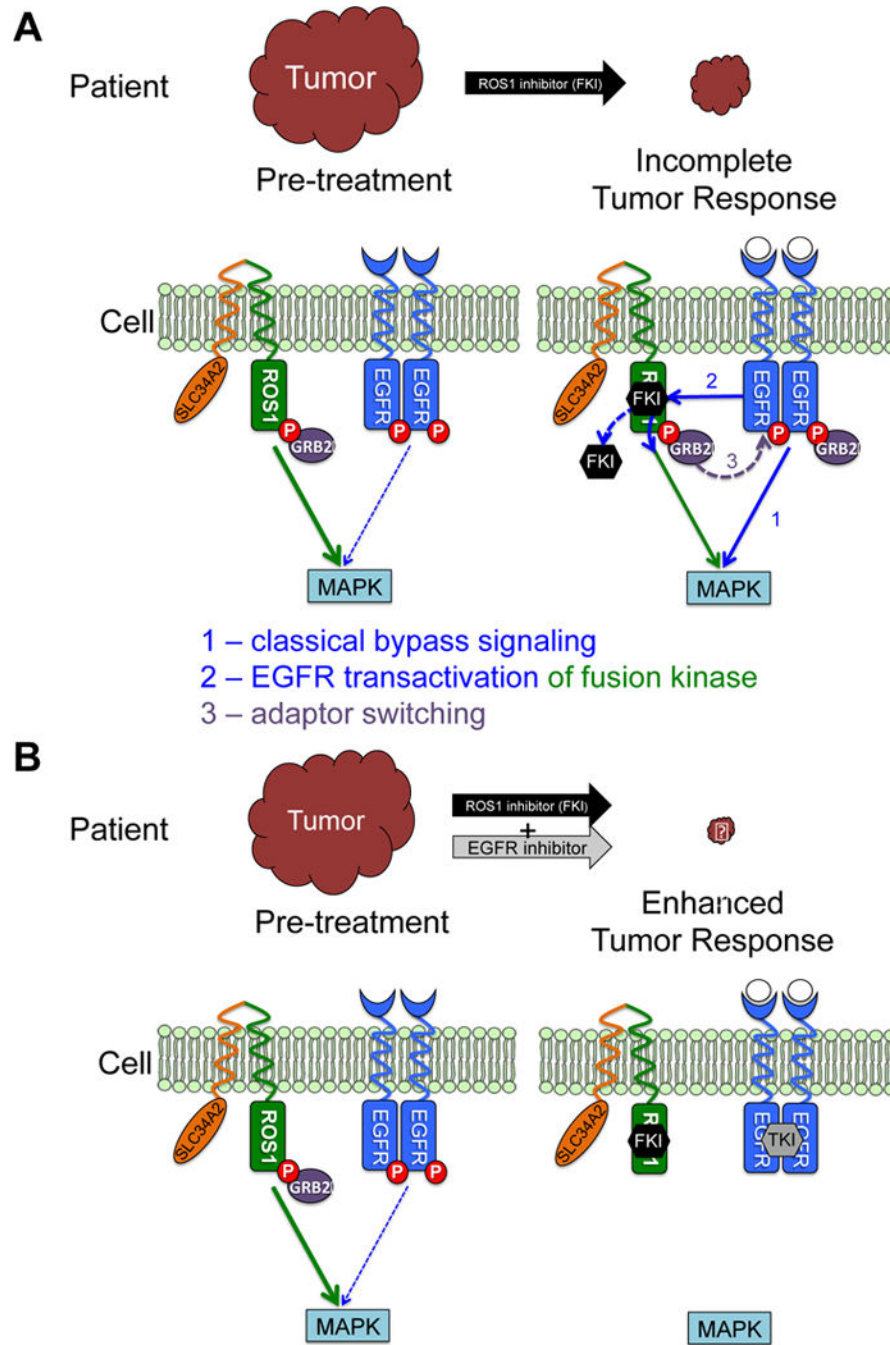


**Figure 6. EGFR and fusion kinase cooperative signaling model**

Cartoon schematic summarizing the three roles described for EGFR in the context of a ROS1 fusion (1) classical by-pass signaling, (2) EGFR transactivation of the fusion kinase, and (3) the observation we describe as adaptor switching using GRB2. We show at the patient level and the cellular level **A**, pre-treatment to incomplete response with FKI only **B**, the enhanced tumor response our work describes using an FKI with an EGFR inhibitor. Our model demonstrates the cooperative signaling that is going on between EGFR and an oncogenic fusion kinase and how the 3 roles we describe for EGFR in this work can only be

blocked with an FKI and an EGFR inhibitor in combination, up-front. FKI = fusion kinase inhibitor.

Author Manuscript

Author Manuscript

Author Manuscript

Author Manuscript